Supporting Information

Electronic Modulation via Asymmetrical Heteronuclear Sites: Unlocking High-Performance Oxidative Dehydrogenation of 1-Butene with CO_2 over VCaOx-FeAlOx Catalysts

Weigao Han[a#], Chao Feng[b#], Shixing Wu[a], Fang Dong[a], Zhicheng Tang[a]*

(a. State Key Laboratory of Low Carbon Catalysis and Carbon Dioxide Utilization, National Engineering Research Center for Fine Petrochemical Intermediates, Lanzhou Institute of Chemical Physics, Chinese Academy of Sciences, Lanzhou 730000, China;

b. College of Chemical and Biological Engineering, Shandong University of Science and Technology, Qingdao, Shandong 266590, China.)

**Corresponding author:*

Tel.: +86–931–4968083, Fax: +86–931–4968019, E–mail address:

tangzhicheng@licp.cas.cn (Z. Tang).

Chemical and materials

Ethanol was purchased from Tianjin Lianlong Bohua Chemical Co. Sodium hydroxide was purchased from Beijing Chemical Factory. Ammonium chloride (cas 12125-02-9) was purchased from Sichuan Xilong Science Co. Nitric acid (cas 7697-37-2) was purchased from Chengdu Kelong Chemical Co. Ferric nitrate (cas 7782-61-8) was purchased from Tianjin Damao Chemical Co. PEO-PPO-PEO (P123) was purchased from SIGMA-ALDRICH (Co.3050). Deionized water was homemade in the laboratory.

Characterization of materials

The morphology of the samples was evaluated with transmission electron microscope (TEM). The images of TEM and selected-area electron diffraction patterns were obtained under a microscope of 200 kV using FEI TECNAIG. Power X-ray diffraction (XRD) analysis was finished at 60 kV and 55 mA with a scanning speed of 0.5° min^{-1}. The 2θ of wide-angle ranged from 10° to 80°. Raman scattering was done by using a Laboratory Human Resources Evolution Raman spectrometer (BX41). The XPS measurement was done on a VG ESCALAB 210 Electron Spectrometer (Mg Kα radiation; hν = 1253.6 eV). The specific surface area and the average pore diameter of the catalysts were measured by nitrogen adsorption with a micromeritics ASAP2010 instrument.

For H_2-TPR, a 40 mg sample was pre-treated at an atmosphere of nitrogen. The

temperature was increased from room temperature to 350 °C with a heating rate of 10 °C min^{-1}. When it cooled down to room temperature, the temperature was increased from room temperature to 900 °C with a heating rate of 10 °C min^{-1}. A reducing gas of 5 % vol. H_2 and 95 % vol. N_2 was passed on the sample at the same time.

For O_2-TPD, an 80 mg sample was pre-treated at an atmosphere of nitrogen. The temperature was increased from room temperature to 300 °C with a heating rate of 10 °C min^{-1}. And it was treated for 90 min. When it cooled down to room temperature, the temperature was increased from room temperature to 50 °C for 60 min with a gas of 5 % vol. O_2 and 95 % vol. N_2 passing through. Finally, the temperature was increased from room temperature to 900 °C with a heating rate of 10 °C min^{-1}.

For CO_2-TPD, an 80 mg sample was pre-treated at an atmosphere of nitrogen. The temperature was increased from room temperature to 300 °C with a heating rate of 10 °C min^{-1}. And it was treated for 90 min. When it cooled down to room temperature, the temperature was increased from room temperature to 50 °C for 60 min with a gas of 5 % vol. CO_2 and 95 % vol. N_2 passing through. Finally, the temperature was increased from room temperature to 900 °C with a heating rate of 10 °C min^{-1}.

For NH_3-TPD, an 80 mg sample was pre-treated at an atmosphere of nitrogen. The temperature was increased from room temperature to 300 °C with a heating rate of 10 °C min^{-1}. And it was treated for 90 min. When it cooled down to room temperature, the temperature was increased from room temperature to 50 °C for 60 min with a gas of 5 % vol. NH_3 and 95 % vol. N_2 passing through. Finally, the

temperature was increased from room temperature to 900 °C with a heating rate of 10 °C min^{-1}.

For 1-butene-TPSR, an 80 mg sample was pre-treated at an atmosphere of nitrogen. The temperature was increased from room temperature to 300 °C with a heating rate of 10 °C min^{-1}. And it was treated for 90 min. When it cooled down to room temperature, the temperature was increased from room temperature to 600 °C with a gas of 1-butene passing through. And the gas was introduced into the mass spectrometer.

For He-coke-TPSR, an 80 mg coked sample was put in program-controlled heating instrument. The temperature was increased from room temperature to 800 °C with a heating rate of 10 °C min^{-1} under a flow of He. And the gas was introduced into the mass spectrometer.

For CO_2-TPO, 40 mg coked sample was put in program-controlled heating instrument. The temperature was increased from room temperature to 800 °C with a heating rate of 10 °C min^{-1} under a flow of CO_2. And the gas was introduced into the mass spectrometer.

TG measurements were made on a NETZSCH STA 449F3 instrument heated from room temperature to 800 °C in the air at 10 °C/min. The elemental compositions of the catalyst samples were analyzed by ICP-OES 730 instrument. (Agilent Co.). Prior to ICP analysis, 20 mg of the catalyst powders was pretreated using 5.0 mL aqua regia solution. The solution was then filtered, diluted, and analyzed after the full digestion.

Table S1. Data of characterization of the $FeAlO_x$, VO_x-$FeAlO_x$, and $VCaO_x$-$FeAlO_x$ samples.

Samples	S_{BET} (m^2/g)[a]	Pore volume/m^3 g^{-1}	Pore Size/nm
$FeAlO_x$	263.06	0.58	8.83
VO_x-$FeCrAlO_x$	121.97	0.42	13.77
$VCaO_x$-$FeCaAlO_x$	87.62	0.40	18.17

Table S2. The percentage of oxygen species by O 1S.

Samples	O_α	O_β	O_γ
$FeAlO_x$	0.13	0.72	0.15
VO_x-$FeAlO_x$	0.13	0.72	0.15
$VCaO_x$-$FeAlO_x$	0.18	0.69	0.13

Table S3. The percentage of base sites by CO_2-TPD.

Samples	Weak basicity	Medium basicity	Strong basicity
$FeAlO_x$	14.11	11.76	74.13
VO_x-$FeAlO_x$	19.81	6.07	74.12
$VCaO_x$-$FeAlO_x$	30.18	12.57	67.25

Table S4. The Bader charge quantification analysis of the $FeAlO_x$ and $VCaO_x$-$FeAlO_x$ samples.

Samples	Electron	Average Bader charge	Average state value
$FeAlO_x$	Fe	6.606	2.787
	Al	0.758	2.710
$VCaO_x$-$FeAlO_x$	Fe	6.645	2.710
	Al	0.765	4.469

Table S5. The Bader charge quantification analysis on different sites of 1-butene before and after adsorption.

Samples	Atom	Bader Charge
Butene	C1	4.107
	C2	4.036
	C4	4.087
	Summary	24
$FeAlO_3$-butene	C1	4.169
	C2	4.078
	C4	4.170
	Summary	23.726
$CaV_2O_4/FeAlO_3$-butene	C1	4.130
	C2	4.073
$FeAlO_3$ site	C4	4.216
	Summary	23.952
$CaV_2O_4/FeAlO_3$-butene	C1	4.130
	C2	4.078
CaV_2O_4 site	C4	4.226
	Summary	23.954

Table S6. The Bader charge quantification analysis on different sites of CO_2 on different sites.

Samples	Atom	Bader Charge
CO_2	O1	4.107
	O2	4.036
	C1	4.087
	Summary	24
CO_2 on $FeAlO_3$ sites	O1	4.169
	O2	4.078
	C1	4.170
	Summary	23.726
CO_2 on $FeAlO_3$ sites of $CaV_2O_4/FeAlO_3$	O1	4.130
	O2	4.073
	C1	4.216
	Summary	23.952
CO_2 on CaV_2O_4 sites of $CaV_2O_4/FeAlO_3$	O1	4.130
	O2	4.078
	C1	4.226
	Summary	23.954

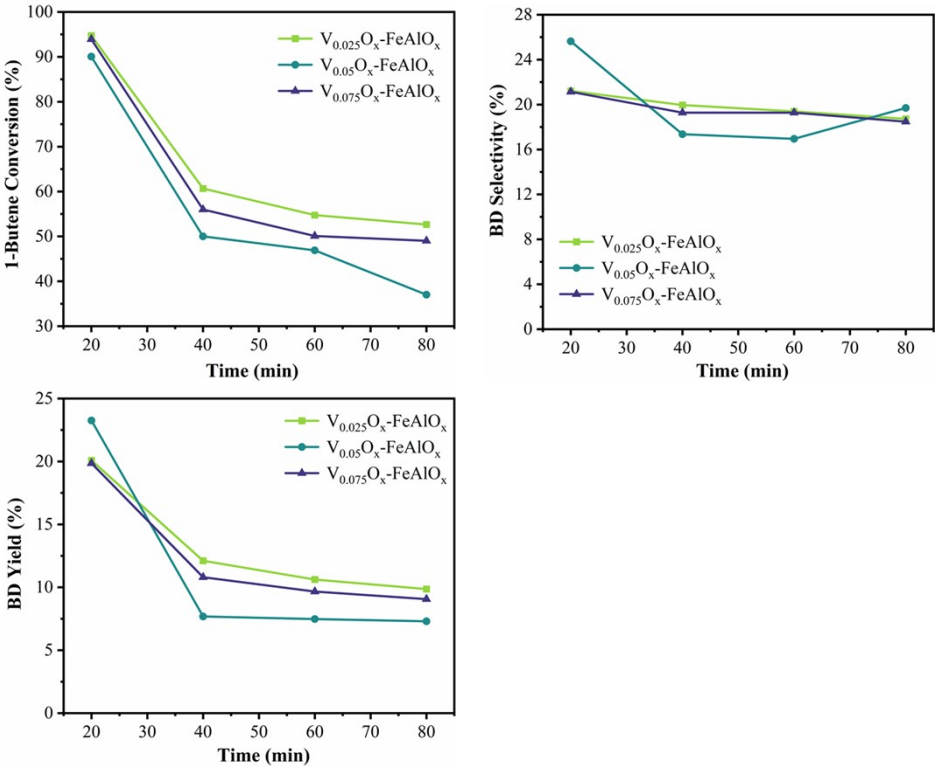

Figure S1. The catalytic performance of VO_x-$FeAlO_x$ catalysts with varying vanadium loadings.

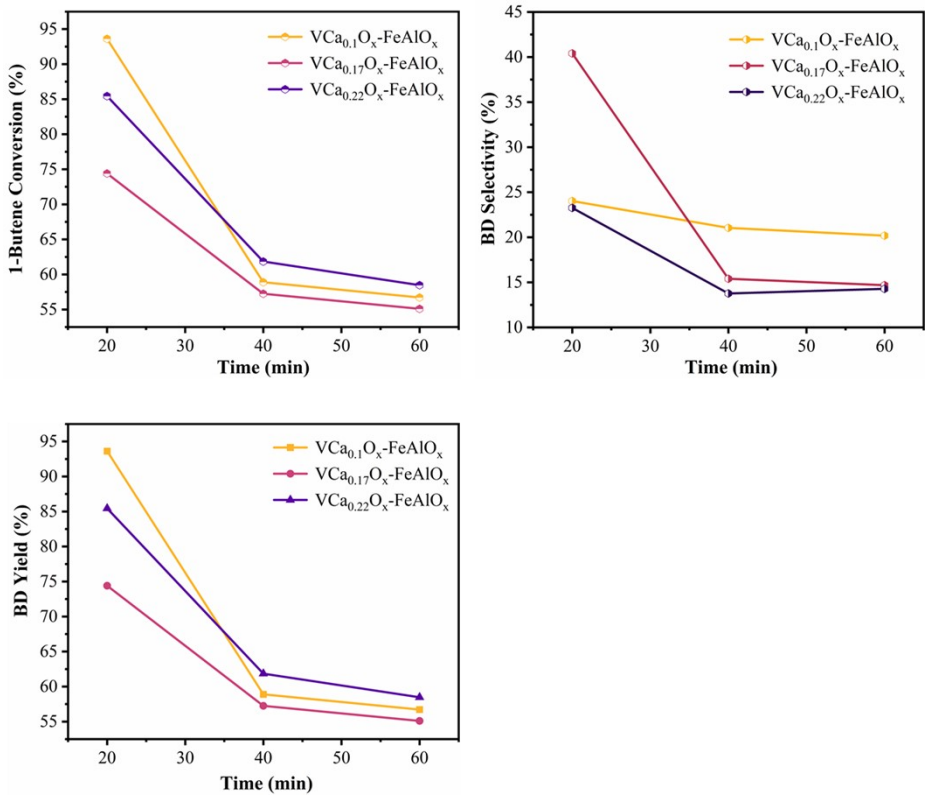

Figure S2. The catalytic performance of VO_x-$FeAlO_x$ catalysts with varying calcium loadings.

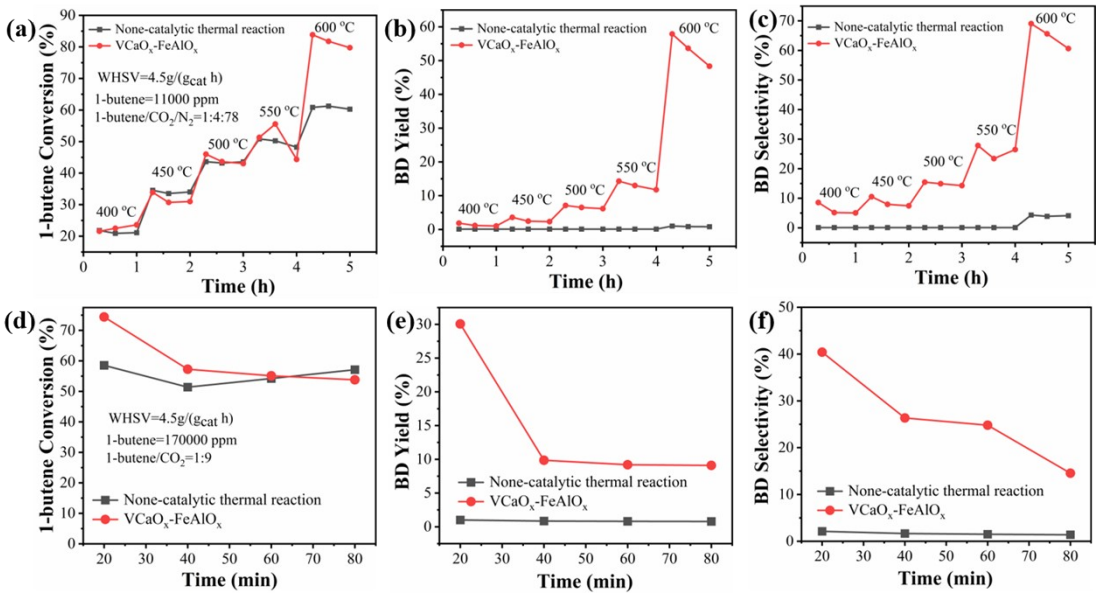

Figure S3 (a) The comparison of 1-butene conversion with none-catalytic thermal reaction and $VCaO_x$-$FeAlO_x$ catalysts, (b) the comparison of BD yield with none-catalytic thermal reaction and $VCaO_x$-$FeAlO_x$ catalysts, (c) the comparison of BD selectivity with none-catalytic thermal reaction and $VCaO_x$-$FeAlO_x$ catalysts (reaction conditions: 60ml/min, 1-butene/CO_2=1:9), (d) the comparison of 1-butene conversion with none-catalytic thermal reaction and $VCaO_x$-$FeAlO_x$ catalysts over different temperatures, (e) the comparison of BD yield with none-catalytic thermal reaction and $VCaO_x$-$FeAlO_x$ catalysts over different temperatures, (f) the comparison of BD selectivity with none-catalytic thermal reaction and $VCaO_x$-$FeAlO_x$ catalysts over different temperatures (reaction conditions: 60ml/min, 1-butene/CO_2/N_2=1:4:78).

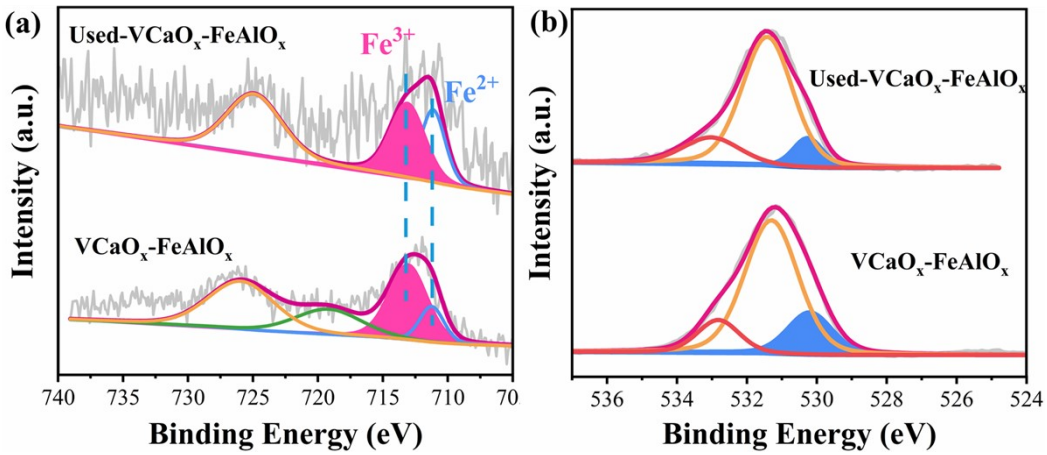

Figure S4. High resolution XPS of Fe 2p and O 1s of the fresh and used $VCaO_x$-$FeAlO_x$ samples

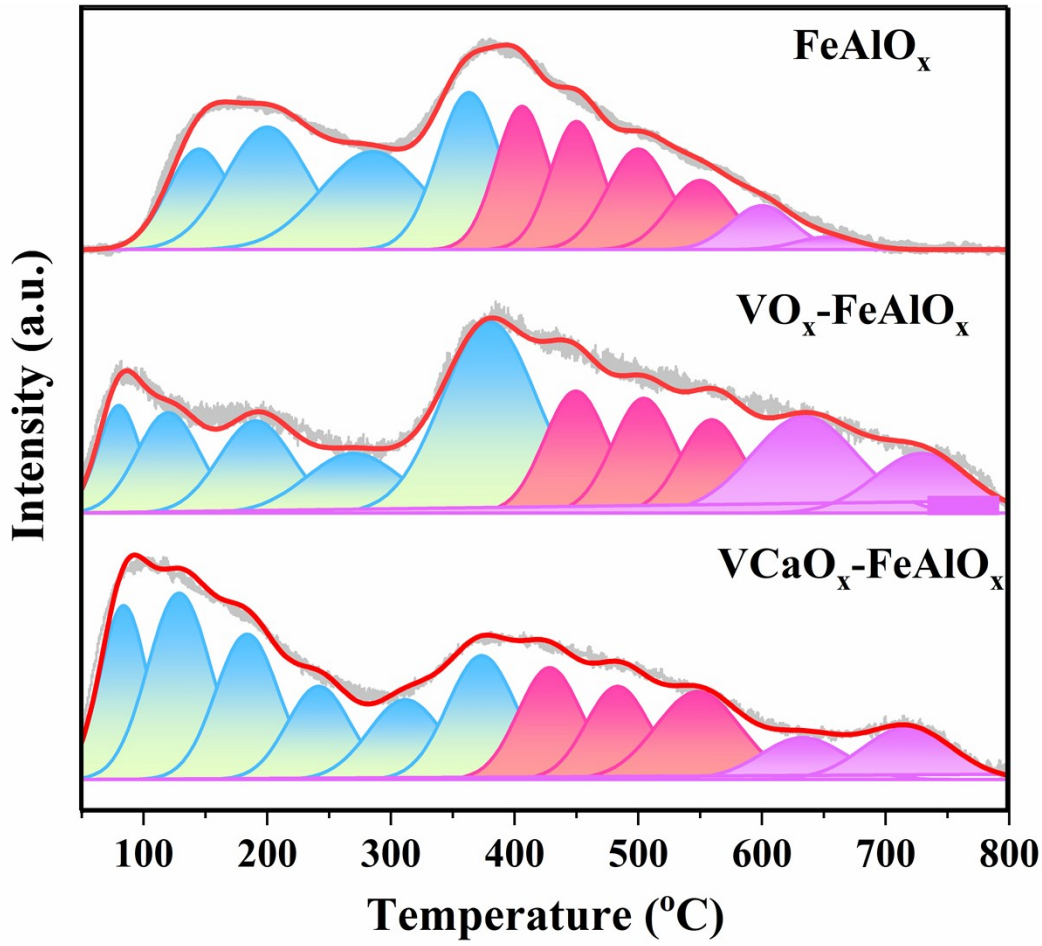

Figure S5. The O_2-TPD curves of $FeAlO_x$, VO_x-$FeAlO_x$ and $VCaO_x$-$FeAlO_x$.

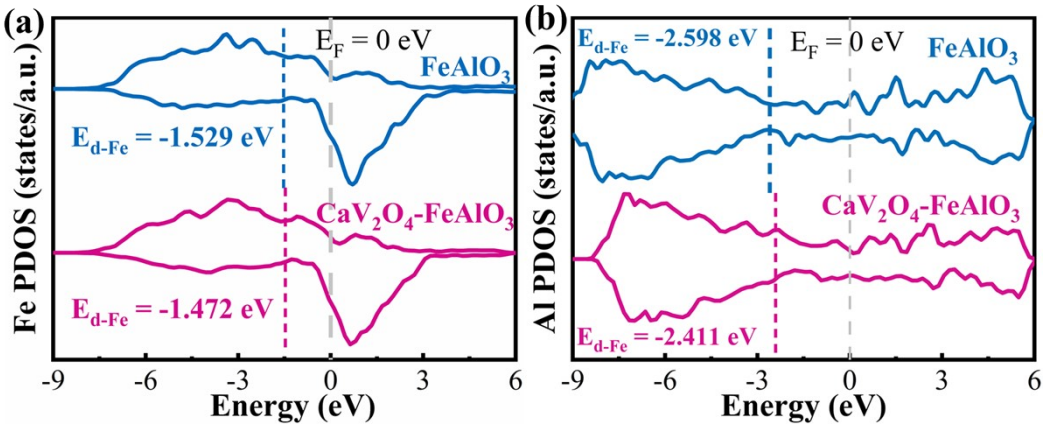

Figure S6. The projected DOS (PDOS) of (a) Fe and (b) Al elements in different structures.

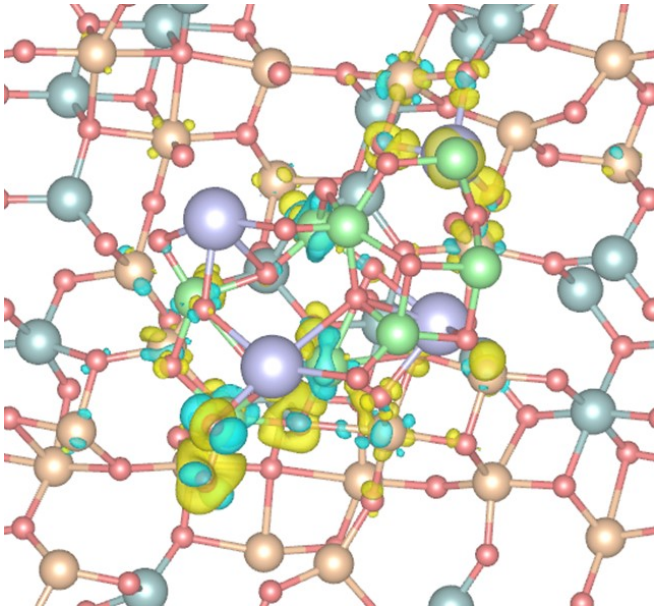

Figure S7. Charge density difference plot for $CaV_2O_4/FeAlO_3$ in above view. The isosurface value is 0.01 e•Bohr-3. Yellow is positive and blue is negative.

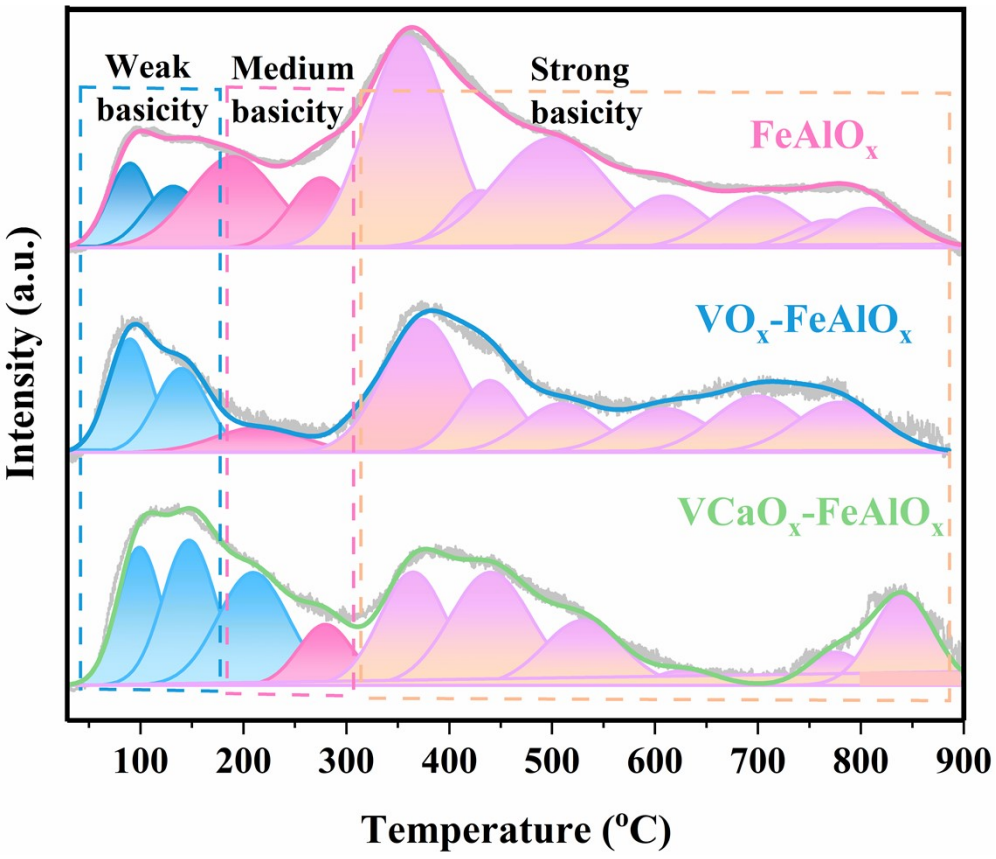

Figure S8. The CO_2-TPD curves of $FeAlO_x$, VO_x-$FeAlO_x$ and $VCaO_x$-$FeAlO_x$ samples.

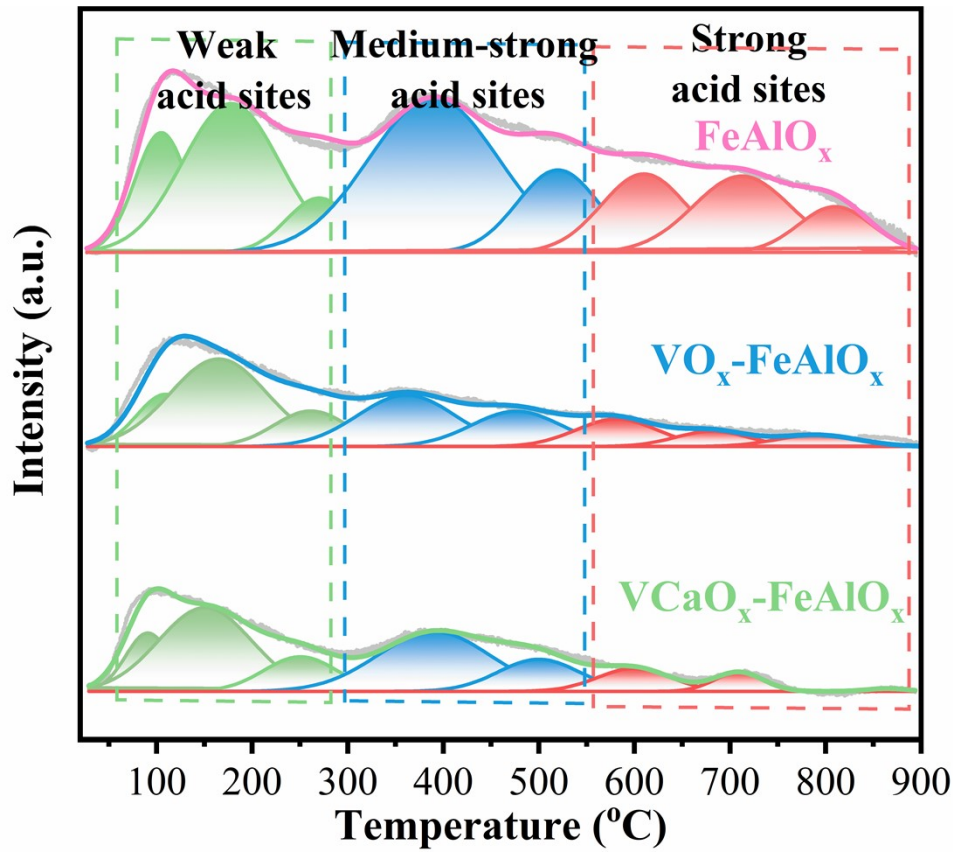

Figure S9. The NH_3-TPD curves of $FeAlO_x$, VO_x-$FeAlO_x$ and $VCaO_x$-$FeAlO_x$ samples.

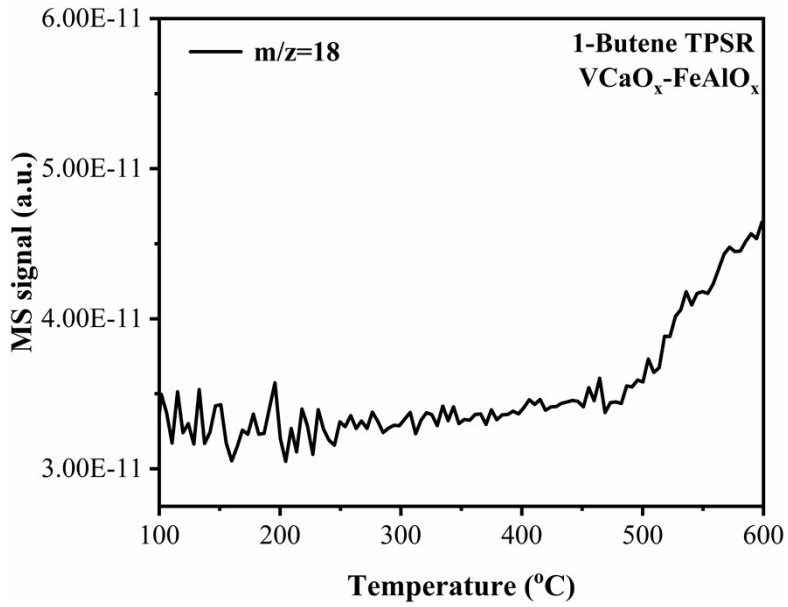

Figure S10. 1-Butene TPSR curve of the $VCaO_x$-$FeAlO_x$ (m/z = 18).

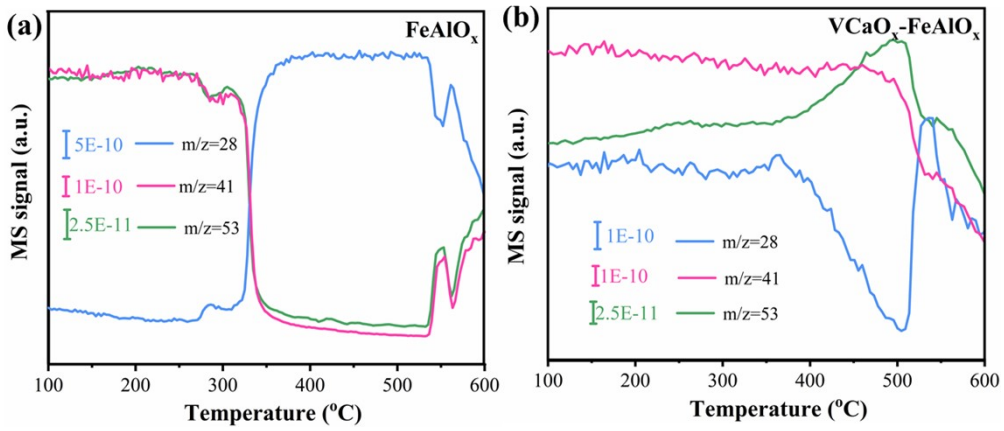

Figure S11. The 1-butene TPSR of (a) $FeAlO_x$ catalysts and (b) $VCaO_x$-$FeAlO_x$ catalysts (m/z=28/41/53)

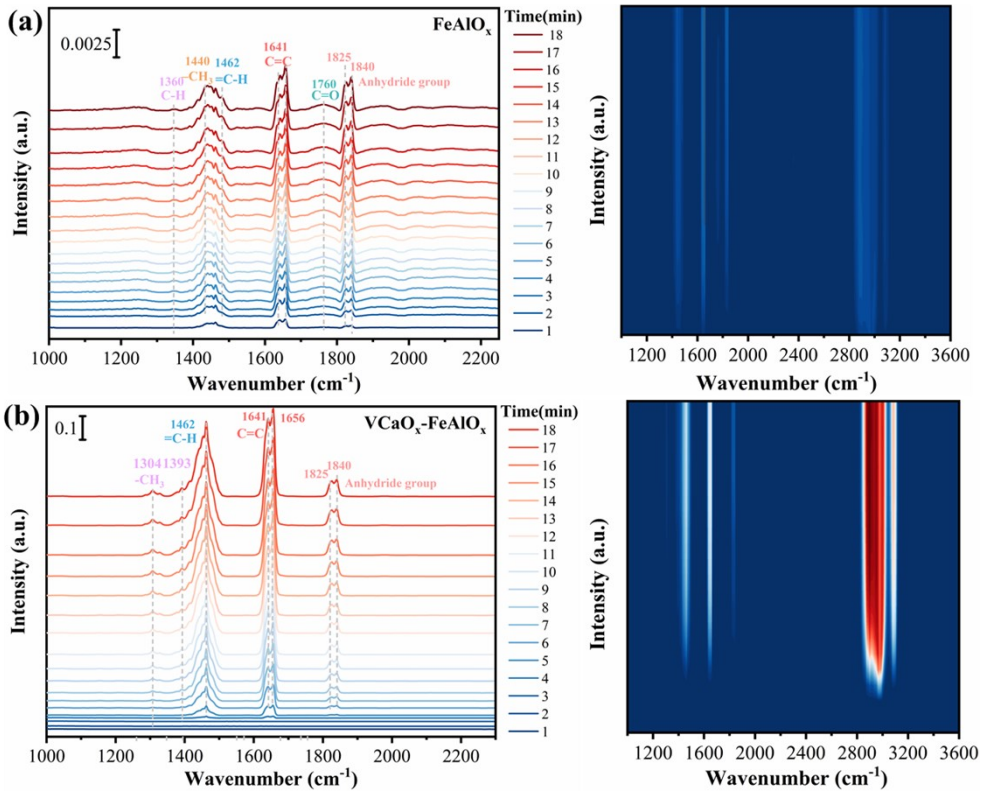

Figure S12. In-situ DRIFT spectra of 1-butene on (a) $FeAlO_x$ and (b) $VCaO_x$-$FeAlO_x$ catalyst at room temperature

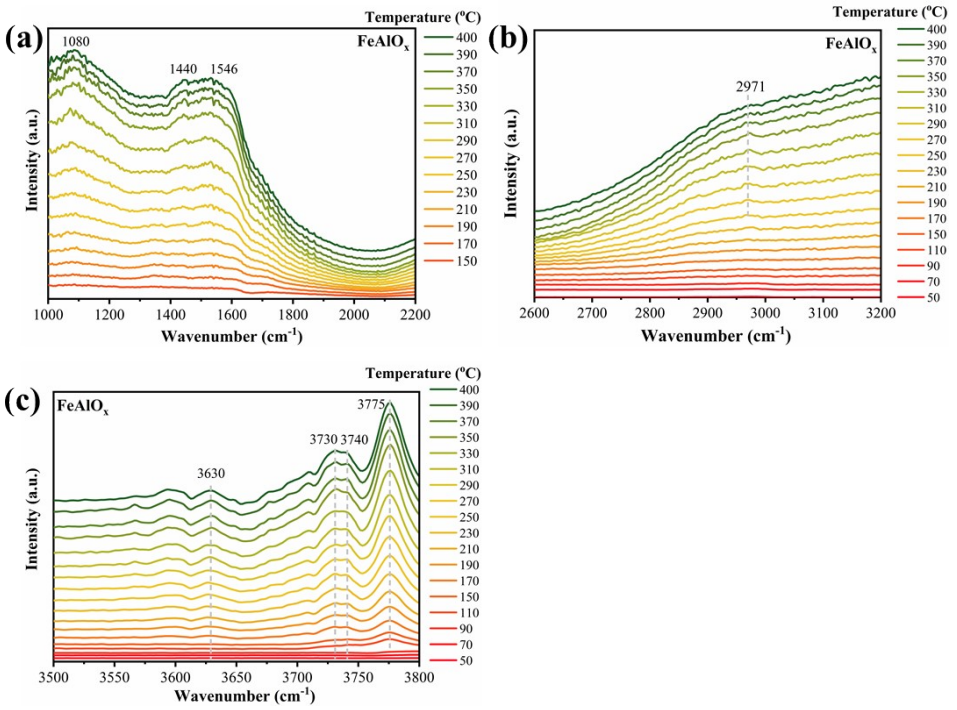

Figure S13. In situ DRIFTS spectra of the $FeAlO_x$ samples exposed to the flow of 1-butene over temperature.

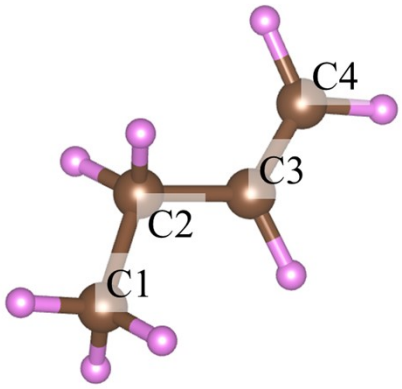

Figure S14. The molecular model of 1-Butene.

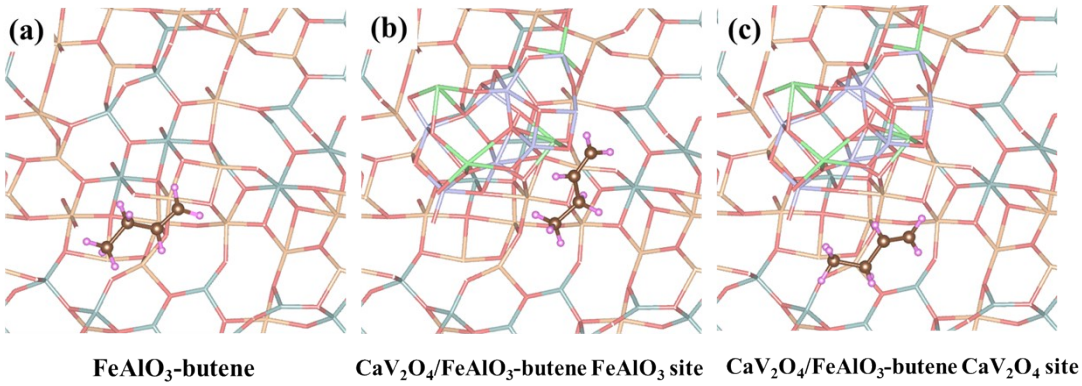

Figure S15. The structure of 1-butene absorbed on different sites.

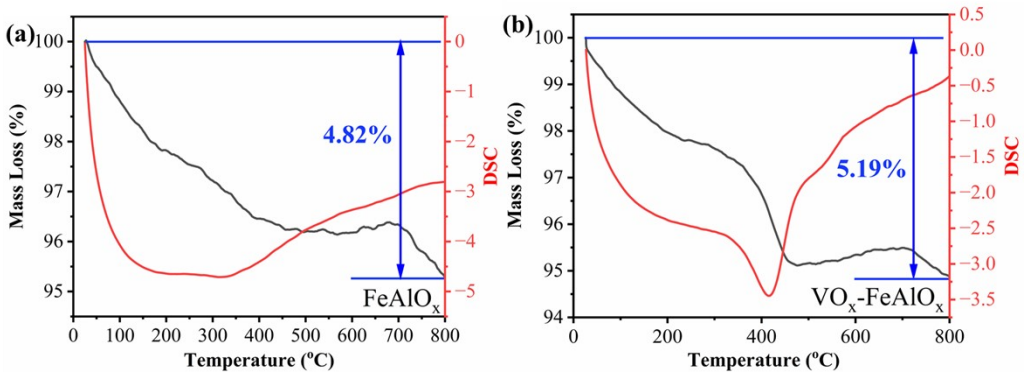

Figure S16. The TG-DSC profile of (a) $FeAlO_x$ and (b) $VCaO_x$-$FeAlO_x$ catalyst.

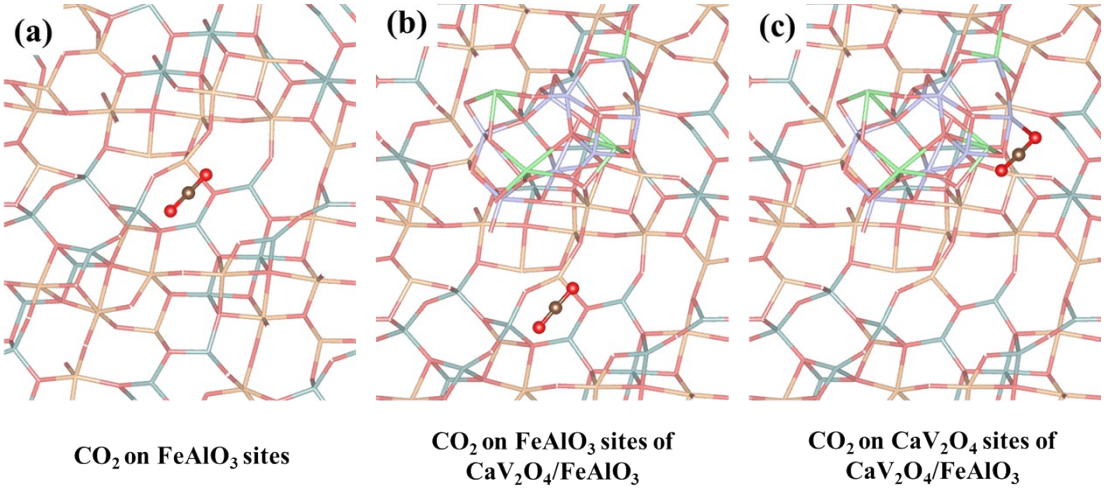

Figure S17. The structure of CO_2 absorbed on different sites.

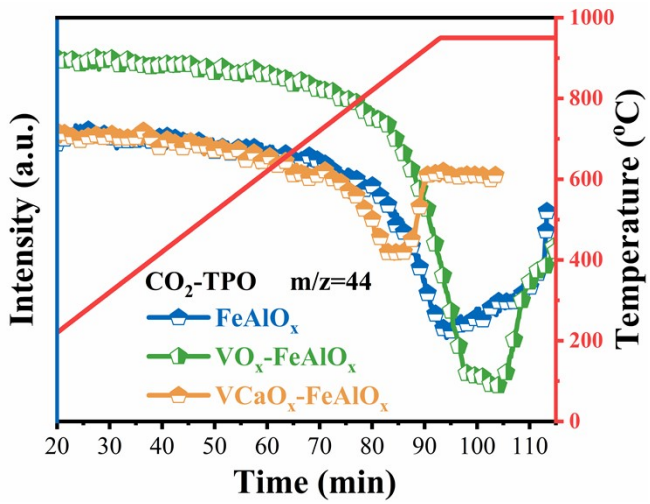

Figure S18. The CO_2-TPO result of FeAlOx, VOx-FeAlOx and VCaOx-FeAlOx catalysts (m/z=44).

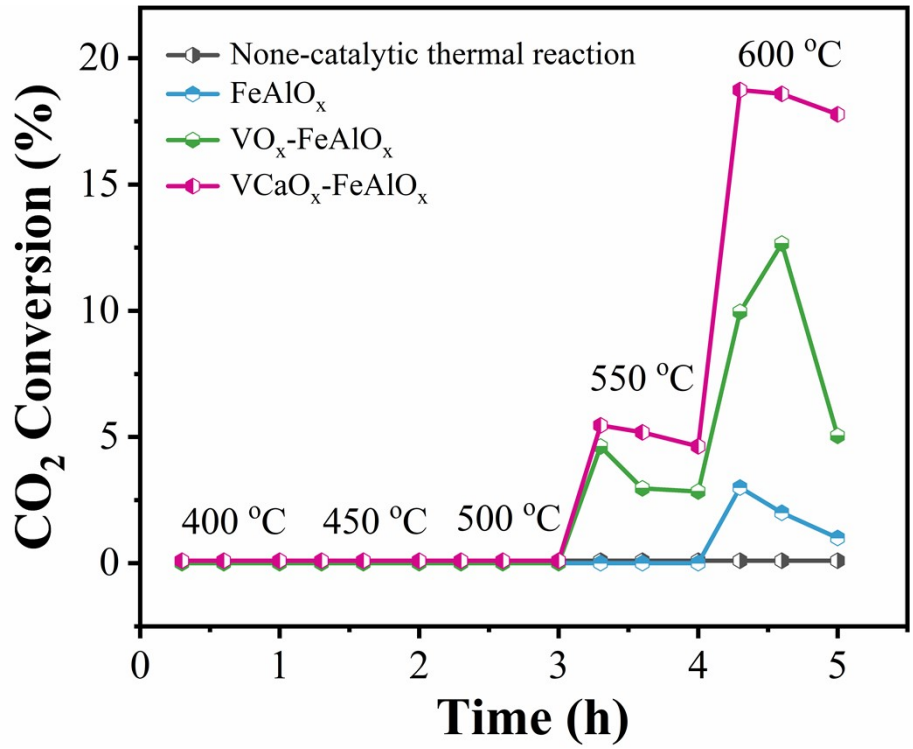

Figure S19. The comparison of CO_2 conversion with thermodynamic equilibrium values, $FeAlO_x$, VO_x-$FeAlO_x$ and $VCaO_x$-$FeAlO_x$ catalysts.

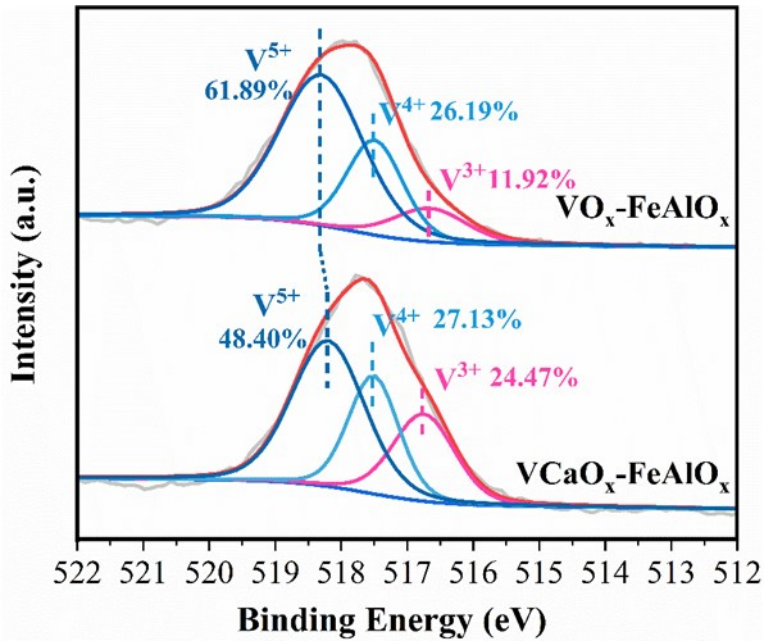

Figure S20. The XPS spectra of V 2p.

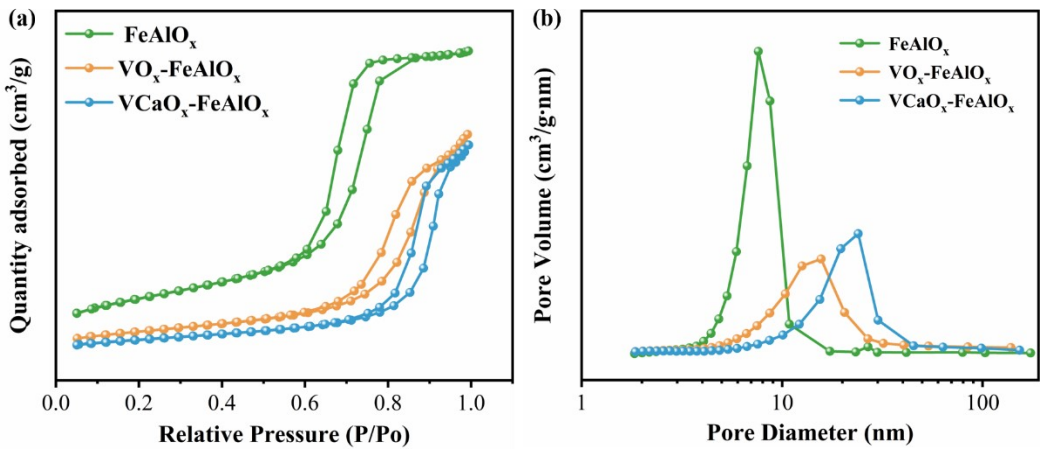

Figure S21. Adsorption-desorption curves (a) and pore-size distributions (b) of $FeAlO_x$, VO_x-$FeAlO_x$, and $VCaO_x$-$FeAlO_x$ samples.